

50.47-Tbit/s Standard Cladding Coupled 4-Core Fiber Transmission over 9,150 km

Daiki Soma, Shohei Beppu, Yuta Wakayama, Seiya Sumita, Hidenori Takahashi, *Member, IEEE*, Noboru Yoshikane, Itsuro Morita, *Fellow, IEEE*, Takehiro Tsuritani, *Senior Member, IEEE*, and Masatoshi Suzuki, *Fellow, IEEE, Fellow, OSA*

Abstract—Since optical submarine cable systems are a part of the global communications infrastructure, their total capacity must be continuously and dramatically enlarged. Recently, methods how to maximize the transmission capacity under electrical power limitations have been studied, and it has been reported that a single band (C-band only) transmission system with more fiber pairs (FPs) could be a promising technology. This finding has triggered work on submarine cables with more FPs. For a further increase in FPs in optical submarine cable systems, which also have space limitations in existing cable designs, space-division multiplexing (SDM) technologies such as multi-core fibers (MCFs) and multi-mode fibers (MMFs) could be promising solutions. In particular, 125- μm standard cladding SDM fibers are attractive for early deployment in submarine cable systems since they are expected to have high productivity and high mechanical reliability similar to existing single-mode fibers (SMFs) with the same cladding diameter. In this paper, we report transpacific MCF transmission over a 30-nm bandwidth using standard cladding ultralow-loss coupled 4-core fibers, extending our previous work. The Q^2 -factors of 608 (4 core \times 152 WDM) SDM/WDM channels modulated with 24-Gbaud DP (dual polarization)-QPSK (quadrature phase shift keying) exceeded the assumed forward error correction (FEC) limits after a 9,150-km transmission. As a result, transmission capacity of 50.47 Tbit/s and a capacity-distance product of 461.8 Pbit/s-km were achieved for standard cladding diameter SDM fibers.

Index Terms— Space-division multiplexing (SDM), Multi-core fiber (MCF), High-capacity transmission, Long-haul transmission, Optical submarine cable system

I. INTRODUCTION

Since optical submarine cable systems are a part of the global communications infrastructure, their total capacity must be continuously and dramatically enlarged to meet the predicted future traffic demands. Recently, methods how to maximize the transmission capacity have been studied under the condition that the electrical power supplied to the system is limited, and it has been reported that a single band (C-band only) transmission system with more fiber pairs (FPs) could be a promising technology [1]. This finding has triggered work on

Some of the research results have been achieved by the Ministry of Internal Affairs and Communications (MIC)/Research and Development of Innovative Optical Network Technology for a Novel Social Infrastructure (JPMI00316) (Technological Theme II: OCEANS), Japan.

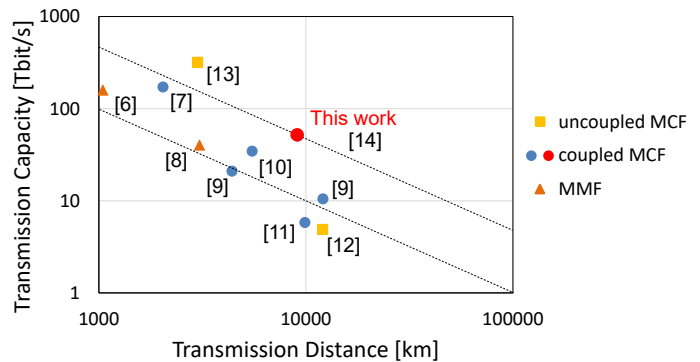


Fig. 1. Relationship between the transmission distance and the transmission capacity reported in recent standard cladding SDM fiber transmission experiments over 1,000 km.

submarine cables with more FPs, and it was announced that the full qualification of submarine repeaters and optical cables containing 20 or more FPs has been completed [2, 3]. For a further increase in FPs in optical submarine cable systems, which also have space limitations in existing cable designs, space-division multiplexing (SDM) technologies such as multi-core fibers (MCFs) and multi-mode fibers (MMFs) could be promising solutions [4]. In particular, 125- μm standard cladding SDM fibers are attractive for early deployment in submarine cable systems since they are expected to have high productivity and high mechanical reliability similar to existing single-mode fibers (SMFs) with the same cladding diameter [5]. Figure 1 shows the relationship between the transmission distance and the transmission capacity reported in recent standard cladding SDM fiber transmission experiments over 1,000 km [6–14]. To date, transoceanic distance transmissions have been reported with standard cladding uncoupled and coupled 4-core fibers [12] and coupled 7-core fibers [9]; however, the bandwidth used in these experiments is a part of the C-band and is smaller than 5 nm. In wide-bandwidth transmission, the longest transmission distance has been 5,500 km in a 34.56-Tbit/s transmission using a coupled 4-core fiber [10].

D. Soma, S. Beppu, Y. Wakayama, S. Sumita, H. Takahashi, N. Yoshikane, I. Morita, T. Tsuritani and M. Suzuki are with KDDI Research, Inc., Fujimino, 356-8502, Japan (e-mail: da-souma@kddi-research.jp; sh-beppu@kddi-research.jp; yu-wakayama@kddi-research.jp; se-sumita@kddi-research.jp; takahashi@kddi-research.jp; yoshikane@kddi-research.jp; morita@kddi-research.jp; tsuri@kddi-research.jp; suzuki@kddi-research.jp).

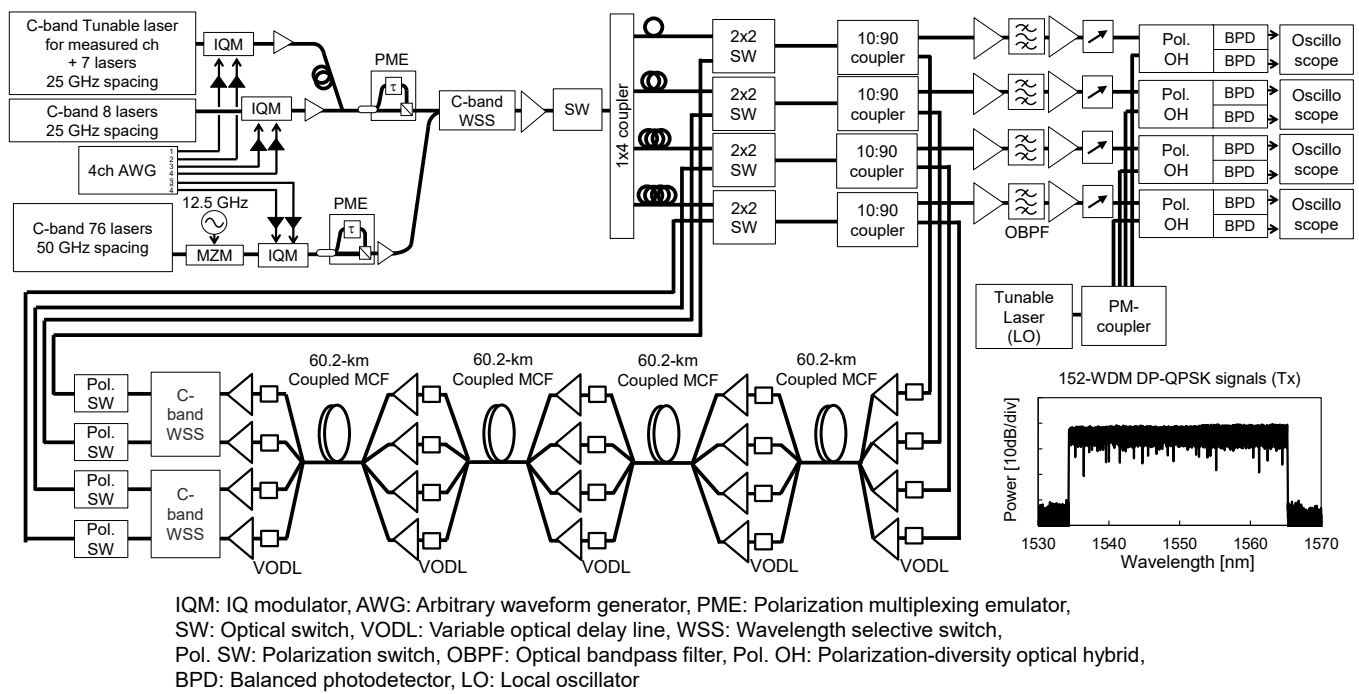


Fig. 2. Experimental setup.

In this paper, we report transpacific MCF transmission over a 30-nm bandwidth using standard cladding ultralow-loss coupled 4-core fibers. This paper extends our previous work [14] with the following additional contributions:

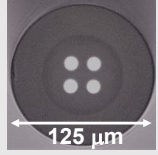
- Detailed description of the experimental setup for a 9,150-km 152 WDM coupled 4-core fiber transmission.
- Evaluation of the tolerance for the nonlinear effects in the coupled MCF to determine the optimal fiber launch power using the center channel of 16-WDM 24-Gbaud DP (dual polarization)-QPSK (quadrature phase shift keying) signals.
- Experimental results of the transmission performance and mode-dependent loss (MDL) as a function of the transmission distance using the typical channels of 152-WDM DP-QPSK signals in the coupled MCF.

Finally, we show the transmission performance of 152-WDM 24-Gbaud DP-QPSK signals with optimal fiber launch power after 9,150-km coupled 4-core fiber transmission. The Q^2 -factors of 608 (4 core \times 152 WDM) SDM/WDM channels exceed the assumed forward error correction (FEC) limits. As a result, transmission capacity of 50.47 Tbit/s and a capacity-distance product of 461.8 Pbit/s-km were achieved for standard cladding diameter SDM fibers.

II. EXPERIMENTAL SETUP

Figure 2 shows the experimental setup for a 9,150-km 152 WDM coupled 4-core fiber transmission. In the transmitter, the continuous wave (CW) lights generated from eight external cavity lasers were combined with a frequency spacing of 50 GHz for even and odd channels. The even and odd channels were independently modulated using a 4-channel arbitrary waveform generator (AWG) and two IQ modulators (IQMs). The IQMs were driven by 24-Gbaud Nyquist-shaped electrical two-level signals for QPSK, which were generated by AWG

TABLE I
OPTICAL CHARACTERISTICS OF COUPLED MCF

Optical characteristics at 1550 nm	
Cross-sectional image	
Core-averaged transmission loss	0.155 dB/km
Effective area	113 μm^2
Core pitch	20.2 μm
Spatial modal dispersion (SMD)	7.1 ps/ $\sqrt{\text{km}}$
Insertion losses of FO devices (lens-coupled type)	0.3 – 0.6 dB
Losses at one splice point	< 0.1 dB
Averaged total span losses	11.8 dB including VODLs

operated at 120 GSamples/s for the I and Q components. Pseudo-random bit sequences (PRBS) with lengths of $2^{15}-1$ were upsampled to two samples/symbol. The delay between two carriers was set to be approximately 10,000 symbols. Following C-band optical amplification, the signals were combined with a 25-GHz spacing and polarization-multiplexed with a delay of 87 ns. Then, we obtained 16 channels of 25-GHz-spaced 24-Gbaud DP-QPSK Nyquist-shaped WDM signals in the C-band.

In addition, we constructed a third rail to load 152 WDM channels in the C-band to maintain not only an optical signal-to-noise ratio (OSNR) but also nonlinear effects in fiber propagation. These 25-GHz spaced 152 tones were generated by a two-cascaded carrier-suppressed modulation of 76 50-GHz-spaced lasers, ranging from 1534.545 nm to 1564.781 nm. These tones were modulated and polarization-multiplexed in the same manner as the measured channel. After three rails were

combined and power-equalized with a C-band wavelength selective switch (WSS), we consequently obtained 152-channel WDM Nyquist-shaped DP-QPSK signals with a bit rate of 96 Gbit/s including the FEC overhead. The inset of Figure 2 shows the measured optical spectrum of the WDM signals. Note that when we measured the BER at every channel, the 16 consecutive channels on the C-band loading rails were automatically disabled, and the measured channel and the 15 dummy channels were tuned to the corresponding frequencies in turn.

The generated WDM signal was split into 4 paths, with a relative delay of 200 ns between subsequent paths for decorrelation, and fed into a recirculating loop system consisting of four spans of 60.2-km coupled 4-core fibers, C-band EDFAs and 2x2 optical switches (SWs). Here, conventional single-mode EDFAs were used to evaluate the transmission potential of coupled MCFs in transpacific transmission. The WDM signals after 4-span transmission were gain-equalized using two 2-channel C-band WSSs. The polarization switches synchronized with the recirculating loop system rotated the polarization state of the signals by 90 degrees per loop to reduce the polarization-dependent loss (PDL). In this experiment, the skew between the four cores, which occurs in all devices in a recirculating loop system, such as FIFO devices, optical amplifiers, WSSs, and optical switches, was compensated for each span via variable optical delay lines (VODLs). The skew contributes to an increase in the required number of MIMO taps in MIMO signal processing, as well as spatial modal dispersion (SMD). Therefore, we constructed the recirculating loop system using optical amplifiers, FIFO devices, and optical patch cords with optical path lengths matched within a few centimeters between the four cores. Moreover, we compensated for the skew on the order of millimeters using the VODLs that can be adjusted up to approximately 6 cm (= 300 ps).

The four cores arranged in a square lattice of the coupled MCF [15] had almost the same refractive index profile as an ultralow-loss pure-silica-core single-mode fiber used for long-haul transmission. Table I shows the optical characteristics at 1550 nm and the cross-sectional image of the fabricated coupled MCF. The core-averaged transmission loss, effective area, core pitch and SMD for the coupled MCF at 1550 nm were approximately 0.155 dB/km, 113 μm^2 , 20.2 μm , and 7.1 ps/ $\sqrt{\text{km}}$, respectively. The insertion losses of the lens-coupled fan-out (FO) devices at 1550 nm ranged from 0.3 to 0.6 dB (including core and individual differences). In addition, the losses at one splice point were less than 0.1 dB for the coupled MCF. Therefore, in this experiment, the averaged total span losses were 11.8 dB, including VODLs with a typical insertion loss of 1.0 dB.

In the receiver, the transmitted WDM signals were detected by four digital coherent receivers based on heterodyne detection with a free-running local oscillator (LO) after channel selection with optical bandpass filters (OBPFs). By using heterodyne detection, the number of photodetectors and A/D converters in the receiver can be reduced to half compared to intradyne

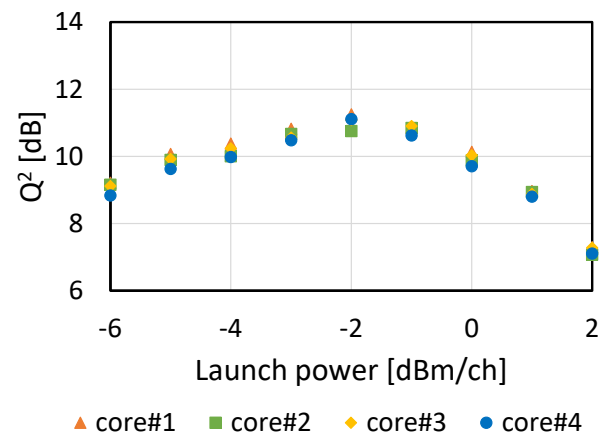


Fig. 3. Q^2 -factors as a function of the fiber launch power at 6,020-km transmission in coupled MCF.

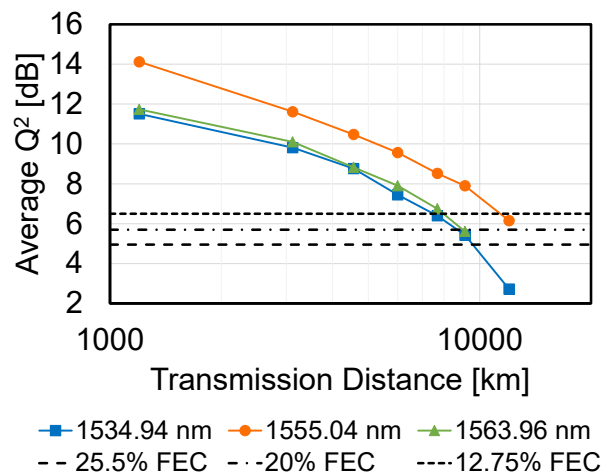


Fig. 4. Q^2 -factors as a function of the transmission distance at 1534.94 nm, 1555.04 nm and 1563.96 nm.

detection. The frequency offset between the LO and the measured signal was adjusted to 20 GHz. The received electrical signals were digitized at 80 GSamples/s using four synchronized real-time oscilloscopes. For offline processing, the stored samples were processed as follows: The samples were downconverted to the base band. After rectangular-shaped Nyquist shaping, the samples for all modes were simultaneously processed by a half-symbol-spaced 8x8 MIMO equalizer with up to 500 taps. The MIMO tap coefficients were updated based on a decision-directed least-mean square (DD-LMS) algorithm [16]. In LMS, data-aided equalization with training signals was used for initial convergence. After that, it was switched to blind equalization (= decision directed mode). After the symbols were decoded, the Q^2 -factors were calculated using only the data after the switch to decision directed mode.

III. RESULTS AND DISCUSSION

A. Fiber launch power optimization

First, we clarified the tolerance for the nonlinear effects in the coupled MCF to determine the optimal fiber launch power. Figure 3 shows the Q^2 -factors as a function of the power per channel at 6,020-km transmission. The fiber launch power was defined as the input power to the FI devices. Here, we used the

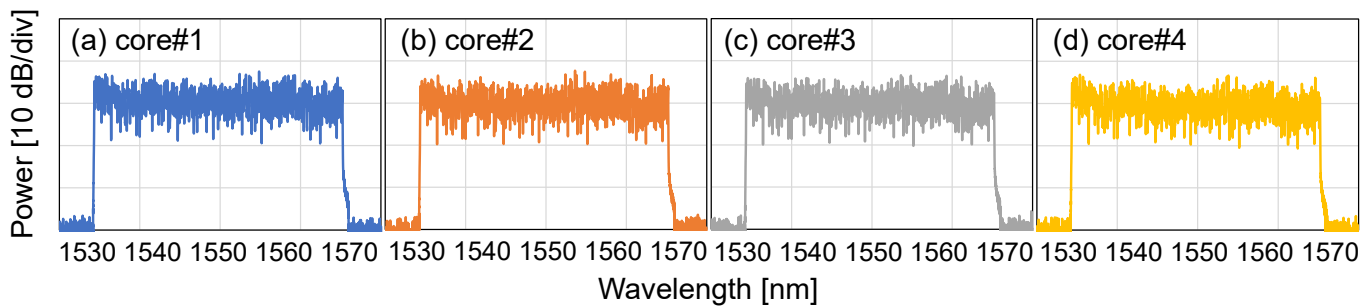


Fig. 5. Optical spectra at (a) core#1, (b) core#2, (c) core#3 and (d) core#4 outputs after 9,150-km transmission (0.02 nm res.).

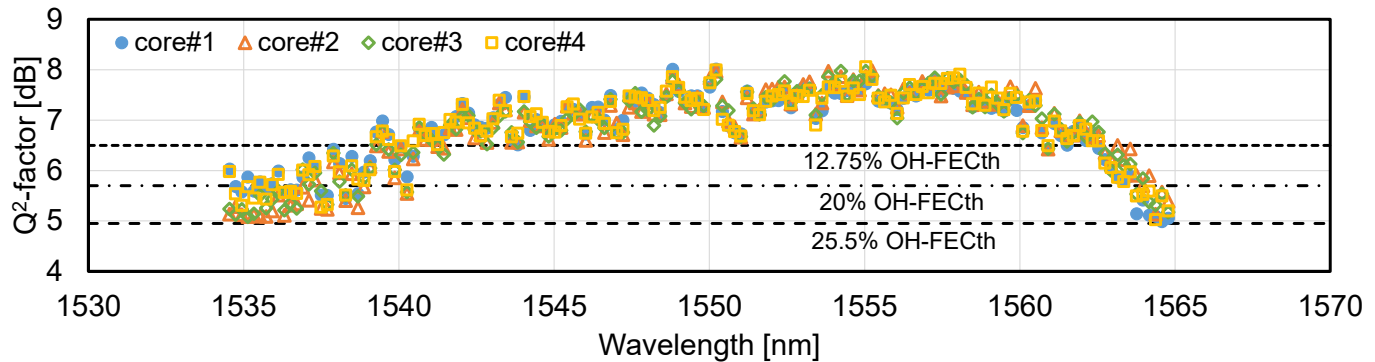


Fig. 6. Q^2 -factors of 608-SDM/WDM channels calculated from the measured BERs.

center channel of 16-WDM 25 GHz-spaced 24-Gbaud DP-QPSK signals, ranging from 1548.615 nm to 1551.620 nm, for the simplification of gain equalization of the transmitted WDM signals using WSSs in the recirculating loop system. The highest Q^2 -factor averaged among the four cores was obtained at -2 dBm/ch. The coupled 4-core fibers had better nonlinear performance since the fiber launch power could be increased compared to the standard cladding uncoupled 4-core fibers with an optimal fiber launch power of -5 dBm/ch [12]. The accumulation of nonlinear noise is suppressed in coupled MCFs compared to uncoupled MCFs and SMFs because the waveform changes along with propagation due to inter-core coupling and mode dispersion [17]. Therefore, the signal powers launched into each core of the coupled 4-core fibers were also adjusted to -2 dBm/ch in the following transpacific transmission experiment using 152-WDM DP-QPSK signals.

B. Transmission performance as a function of the transmission distance

Next, the Q^2 -factors as a function of the transmission distance in the typical three channels, which are the center channel and two channels at both edges in the 152-WDM signals with a bandwidth of 30 nm, were measured to clarify the reachability of the 152-WDM DP-QPSK signals in the coupled MCF. Figure 4 shows the relationship between the transmission distance and the core-averaged Q^2 -factors at wavelengths of 1534.94 nm, 1555.04 nm, and 1563.96 nm. In this experimental setup, the Q^2 -factors of the two channels at both edges degraded by approximately 2 dB at each transmission distance compared to the center channel. In addition, the Q^2 -factors of the two channels at both edges exceeding the FEC threshold of 25.5% [18], which has the largest overhead among the FECs assumed this time, were obtained after 9,150-km transmission. Therefore,

the transmission distance was set to 9,150 km in the following high-capacity transmission experiment using 152-WDM DP-QPSK signals.

C. Transmission performance of 152-WDM DP-QPSK signals over coupled 4-core fiber

Finally, we evaluated the transmission performance of 152-WDM DP-QPSK signals after 9,150-km coupled 4-core fiber transmission. Figures 5 (a)–(d) show the optical spectra at the output of each core after 9,150-km transmission ((a) core #1, (b) core #2, (c) core #3, and (d) core #4). The flattened and stable WDM channels were maintained across a 30-nm bandwidth in the C-band after transmission due to gain equalization using WSSs in the recirculating loop system, although core-to-core coupling occurs dynamically in coupled MCFs. In addition, the power fluctuation among the cores in each WDM channel was very small because no significant difference was observed in the optical spectra between the four cores, as shown in Figure 5.

Figure 6 shows the Q^2 -factors of 608 (4 core \times 152 WDM) SDM/WDM channels calculated from the measured BERs. In this experiment, we assumed a rate-adaptive FEC [19] (multirate FEC [20]), which is a promising technology used to maximize system capacity with the OSNR and the nonlinear effect variation between WDM channels. The assumed three different soft-decision (SD)-FECs based on low-density parity-check (LDPC) codes with a 12.75% overhead (OH) and 6.5 dB FEC limit [21], a 20% OH and 5.7 dB FEC limit [22], and a 25.5% OH and 4.95 dB FEC limit [18] were employed, and one of them was selected for each channel according to the measured BERs. From the results shown in Figure 6, the Q^2 -factors of 107 WDM channels, 19 WDM channels, and 26 WDM channels exceeded the thresholds of 12.75% OH FEC,

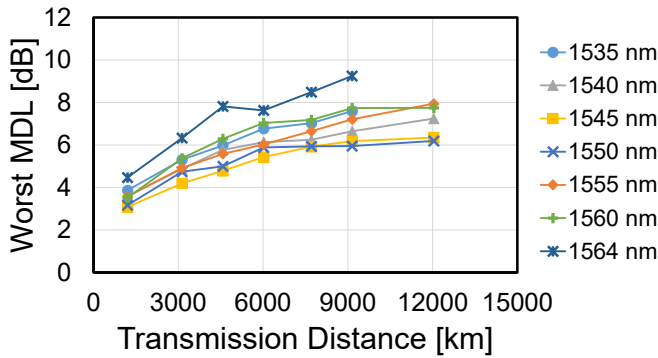


Fig. 7. Relationship between transmission distance and worst MDL.

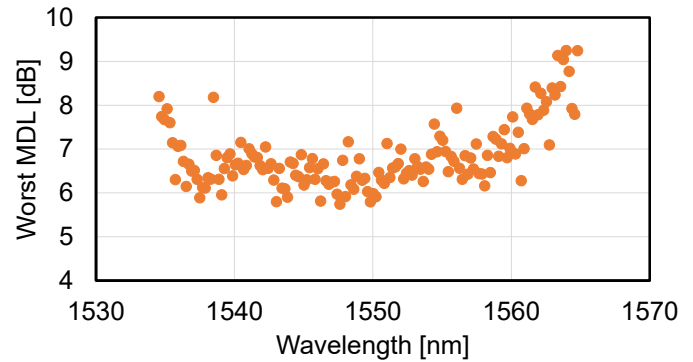


Fig. 8. Worst MDLs of each WDM channel.

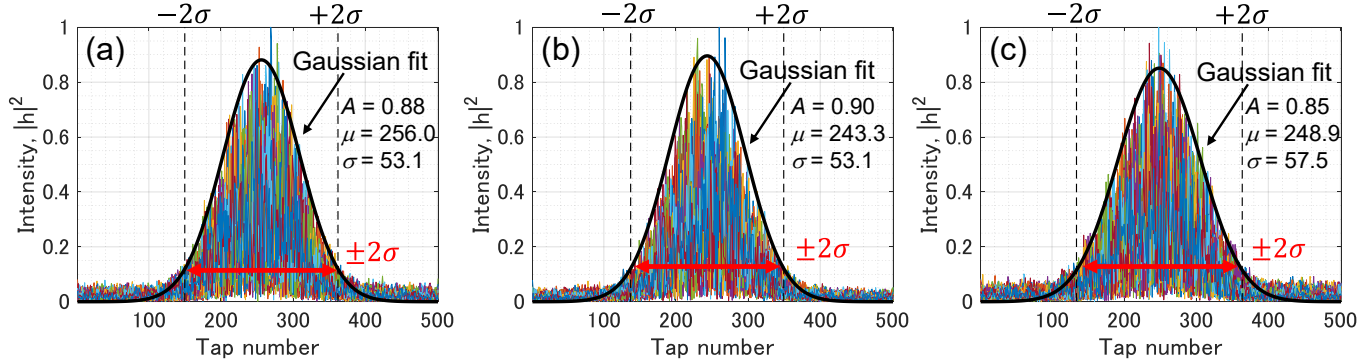


Fig. 9. MIMO impulse responses at (a) 1534.545 nm, (b) 1550.016 nm, and (c) 1564.781 nm after the 9,150-km transmission.

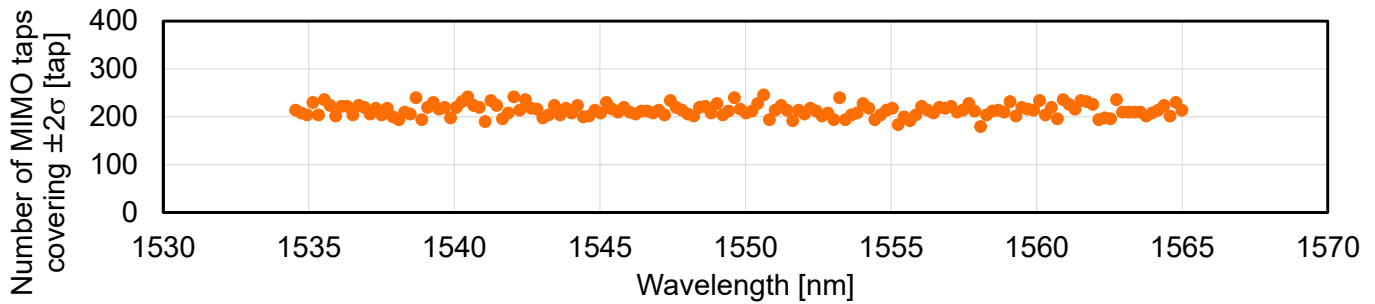


Fig. 10. Relationship between the wavelength and the number of 8x8 MIMO taps covering $\pm 2\sigma$ of the Gaussian fitting of the MIMO impulse response.

20% OH FEC, and 25.5% OH FEC, respectively. The worst Q^2 -factor was 4.98 dB at 1564.577 nm for core #1, which was higher than the FEC limit of 4.95 dB for the 25.5% OH FEC. The maximum difference in the Q^2 -factors between the 4 cores in each WDM channel was 0.9 dB at 1534.545 nm.

Figure 7 shows the relationship between the transmission distance and largest MDL [9] in seven typical channels. The largest MDL is the difference between the maximum and minimum singular values among 8 tributaries (4-spatial tributaries x 2 polarizations) averaged over the 24 GHz signal bandwidth. The MDL increased with increasing transmission distance and tended to be relatively large at both edges of the C-band, especially at longer wavelengths. In addition, the MDL would be enhanced compared to a straight-line configuration as well as the PDL [23] because the signal lights pass through the same devices in each loop in the recirculating loop system. Figure 8 shows the largest MDLs between the 8 tributaries of each WDM channel after the 9,150-km transmission. The MDL is caused by the loss difference between the cores and the wavelength dependence of the optical amplifiers, VODLs, WSSs, polarization switches, and optical switches in the

recirculating loop system. The largest MDLs increased in several channels at both edges of the 30-nm bandwidth due to the large difference among the four cores in the gain of the amplifiers for the recirculating loop system at both edges of the C-band. Figure 9 shows the MIMO impulse responses and their Gaussian fitting at (a) 1534.545 nm, (b) 1550.016 nm, and (c) 1564.781 nm after the 9,150-km transmission. The Gaussian fitting given by $f(x; A, \mu, \sigma) = Ae^{-\frac{(x-\mu)^2}{2\sigma^2}}$ was obtained by calculating the square of the intensity of the 8x8 MIMO impulse response and averaging it over 64 elements in the 8x8 MIMO matrix [24]. Note that no wavelength dependency was observed in these MIMO impulse responses. To roughly estimate how many MIMO taps should be set, Figure 10 shows the number of 8x8 MIMO taps covering $\pm 2\sigma$ of the Gaussian fitting of the MIMO impulse response as shown in Figure 9 in each WDM channel. These MIMO tap numbers were less than 300 across the 30-nm bandwidth in the C-band after the 9,150-km transmission, although the number increased with increasing square root of the transmission distance in the coupled MCF [25].

From the obtained experimental results, a transmission capacity of 50.47 Tbit/s (12.62 Tbit/s/core) was achieved using the 152-WDM 24-Gbaud DP-QPSK signals over a 30-nm bandwidth after a 9,150-km transmission by assuming the rate-adaptive FEC.

IV. CONCLUSION

We clarified the tolerance for the nonlinear effects in the coupled MCF to determine the optimal fiber launch power. 50.47-Tbit/s transpacific coupled MCF transmission over a 30-nm bandwidth has been successfully demonstrated using standard cladding ultralow-loss coupled 4-core fibers. The Q^2 -factors of all 608 SDM/WDM channels modulated with 24-Gbaud DP-QPSK exceeded the assumed multirate FEC limits after a 9,150-km transmission.

ACKNOWLEDGMENT

We would like to thank the staff of Sumitomo Electric Industries, Ltd. and Optoquest Co., Ltd. for their assistance in this study.

REFERENCES

- [1] J. D. Downie, "Maximum Capacities in Submarine Cables With Fixed Power Constraints for C-Band, C+L-Band, and Multicore Fiber Systems," *Journal of Lightwave Technology*, Volume 36, Issue 18, pp. 4025 – 4032, Sept. 15, (2018).
- [2] NEC Press Releases, "NEC qualifies 20 fiber pair subsea telecom cable systems, with further advances soon," (2020).
- [3] SubCom Press Releases, "SubCom achieves qualification for High Fiber Count (HFC) cable, begins manufacturing," (2019).
- [4] J. D. Downie, X. Liang, and S. Makovejs, "ON THE POTENTIAL APPLICATION SPACE OF MULTICORE FIBRES IN SUBMARINE CABLES," ECOC2019, M.1.D.4, (2019).
- [5] T. Matsui, T. Kobayashi, H. Kawahara, E. L. T. de Gabory, T. Nagashima, T. Nakanishi, S. Saitoh, Y. Amma, K. Maeda, S. Arai, R. Nagase, Y. Able, S. Aozasa, Y. Wakayama, H. Takeshita, T. Tsuritani, H. Ono, T. Sakamoto, I. Morita, Y. Miyamoto, and K. Nakajima, "118.5 Tbit/s Transmission over 316 km-Long Multi-Core Fiber with Standard Cladding Diameter," OECC2017, PDP2, (2017).
- [6] G. Rademacher, R. S. Luis, B. J. Puttnam, T. A. Eriksson, E. Agrell, R. Maruyama, K. Aikawa, H. Furukawa, Y. Awaji, and N. Wada, "159 Tbit/s C+L Band Transmission over 1045 km 3-Mode Graded-Index Few-Mode Fiber," OFC2018, Th4C.4, (2018).
- [7] G. Rademacher, R. S. Luis, B. J. Puttnam, R. Ryf, S. van der Heide, T. A. Eriksson, N. K. Fontaine, H. Chen, R.-J. Essiambre, Y. Awaji, H. Furukawa, and N. Wada, "172 Tb/s C+L Band Transmission over 2040 km Strongly Coupled 3-Core Fiber," OFC2020, Th4C.5, (2020).
- [8] K. Shibahara, T. Mizuno, H. Kawakami, T. Kobayashi, M. Nakamura, K. Shikama, K. Nakajima, and Y. Miyamoto, "3-Mode Transmission with 40.2-Tb/s Capacity Using Cyclic Mode Permutation," OFC2019, W3F.2, (2019).
- [9] R. Ryf, J. C. Alvarado-Zacarias, S. Wittek, N. K. Fontaine, R.-J. Essiambre, H. Chen, R. Amezcua-Correa, H. Sakuma, T. Hayashi, and T. Hasegawa, "Coupled-Core Transmission over 7-Core Fiber," OFC2019, Th4B.3, (2019).
- [10] R. Ryf, J. C. Alvarado, B. Huang, J. Antonio-L'opez, S. H. Chang, N. K. Fontaine, H. Chen, R.-J. Essiambre, E. Burrows, R. Amezcua-Correa, T. Hayashi, Y. Tamura, T. Hasegawa, and T. Taru, "Long-Distance Transmission over Coupled-Core Multicore Fiber," ECOC2016, Th.3.C.3, (2016).
- [11] R. Ryf, N. K. Fontaine, S. H. Chang, J. C. Alvarado, B. Huang, J. Antonio-L'opez, H. Chen, R.-J. Essiambre, E. Burrows, R. W. Tkach, R. Amezcua-Correa, T. Hayashi, Y. Tamura, T. Hasegawa, and T. Taru, "Long-Haul Transmission over Multi-Core Fibers with Coupled Cores," ECOC2017, M.2.E.1, (2017).
- [12] D. Soma, S. Beppu, H. Takahashi, N. Yoshikane, I. Morita, and T. Tsuritani, "Performance Comparison for Standard Cladding Ultra-Low-Loss

- Uncoupled and Coupled 4-Core Fibre Transmission over 15,000 km," ECOC2020, Mo2E.4, (2020).
- [13] B. J. Puttnam, R. S. Luis, G. Rademacher, Y. Awaji, and H. Furukawa, "319 Tb/s Transmission over 3001 km with S, C and L band signals over >120nm bandwidth in 125 μ m wide 4-core fiber," OFC2021, F3B.3, (2021).
- [14] D. Soma, S. Beppu, Y. Wakayama, S. Sumita, H. Takahashi, N. Yoshikane, I. Morita, T. Tsuritani, and M. Suzuki, "50.47-Tbit/s Standard Cladding Ultra-Low-Loss Coupled 4-Core Fiber Transmission over 9,150 km," OFC2021, W7D.3, (2021).
- [15] H. Sakuma, T. Hayashi, T. Nagashima, T. Nakanishi, D. Soma, T. Tsuritani, and T. Hasegawa, "MICROBENDING BEHAVIOR OF RANDOMLY-COUPLED ULTRA-LOW-LOSS MULTI-CORE FIBER," ECOC2019, M.1.D.2, (2019).
- [16] Y. Mori, Z. Chao, and K. Kikuchi, "Novel FIR-Filter Configuration Tolerant to Fast Phase Fluctuations in Digital Coherent Receivers for Higher-order QAM signals," OFC2012, OTh4C.4, (2012).
- [17] C. Antonelli, A. Mecozzi, and M. Shttaif, "Scaling of inter-channel nonlinear interference noise and capacity with the number of strongly coupled modes in SDM systems," OFC2016, W4I.2, (2016).
- [18] K. Sugihara, Y. Miyata, T. Sugihara, K. Kubo, H. Yoshida, and W. Matsumoto, "A Spatially-coupled Type LDPC Code with an NCG of 12 dB for Optical Transmission beyond 100 Gb/s," OFC2013, OM2B.4, (2013).
- [19] D. Zou, and I. B. Djordjevic, "FPGA-based Rate-adaptive LDPC-coded Modulation for the Next Generation of Optical Communication Systems," *Opt. Express*, 24(18), 21159, (2016).
- [20] OIF technical white paper, Flex Coherent DWDM Transmission Framework Document, "https://www.oiforum.com/wp-content/uploads/2019/01/OIF-FD-FLEXCOH-DWDM-01.0-1.pdf," (2017).
- [21] T. Kobayashi, M. Nakamura, F. Hamaoka, K. Shibahara, T. Mizuno, A. Sano, H. Kawakami, A. Isoda, M. Nagatani, H. Yamazaki, Y. Miyamoto, Y. Amma, Y. Sasaki, K. Takenaga, K. Aikawa, K. Saitoh, Y. Jung, D. J. Richardson, K. Pulverer, M. Bohn, M. Nooruzzaman, and T. Morioka, "1-Pb/s (32 SDM/46 WDM/768 Gb/s) C-band Dense SDM Transmission over 205.6-km of Single-mode Heterogeneous Multi-core Fiber using 96-Gbaud PDM-16QAM Channels," OFC2017, Th5B.1, (2017).
- [22] D. Chang, F. Yu, Z. Xiao, N. Stojanovic, F. N. Hauske, Y. Cai, C. Xie, L. Li, X. Xu, and Q. Xiong, "LDPC Convolutional Codes Using Layered Decoding Algorithm for High-speed Coherent Optical Transmission," OFC2012, OW1H.4, (2012).
- [23] C. Vinegoni, M. Karlsson, M. Petersson, and H. Sunnerud, "The Statistics of Polarization-Dependent Loss in a Recirculating Loop," *Journal of Lightwave Technology*, Volume 22, Issue 4, pp. 968 – 976, May 4, (2004).
- [24] A. Mecozzi, C. Antonelli, and M. Shttaif, "Intensity impulse response of SDM links," *Opt. Express*, 23(5), 5738, (2015).
- [25] S. Beppu, D. Soma, H. Takahashi, N. Yoshikane, I. Morita, and T. Tsuritani, "Experimental Verification on Digital Back Propagation Gain in MCF transmission over 6020-km Uncoupled and Coupled 4-Core Fibres," ECOC2020, Mo2E-2, (2020).

Daiki Soma received B.E. and M.E. degrees in information science and technology from Hokkaido University, Sapporo, Japan, in 2010 and 2012, respectively. He joined KDDI Corporation, Tokyo, Japan, in 2012. Since 2013, he has been working with KDDI R&D Laboratories, Inc. (currently KDDI Research, Inc.), Saitama, Japan, and has been engaged in research on space division multiplexed optical fiber transmission systems. He was a recipient of the 2017 IEICE Communications Society OCS Young Researchers Award in 2017, the Young Researcher's Award of IEICE in 2018, and the 2020 IEICE Communications Society OCS Best Paper Award.

Shohei Beppu received B.E. and M.E. degrees in communication engineering from Tohoku University, Miyagi, Japan, in 2013 and 2015, respectively. He joined KDDI Corporation, Tokyo, Japan, in 2015. Since 2016, he has been working with KDDI R&D Laboratories, Inc. (currently KDDI Research, Inc.), Saitama, Japan. His current research interests include signal processing for coherent optical communication

systems and space-division-multiplexed optical transmission systems.

Yuta Wakayama received M.E. and Ph.D. degrees in information science and technology from Hokkaido University, Sapporo, Japan, in 2010 and 2013, respectively.

After graduation, he joined KDDI Corporation, Tokyo, Japan. Since 2014, he has been with KDDI R&D Laboratories (currently KDDI Research), Inc., Saitama, Japan. His research interests include space-division-multiplexed optical fiber transmission systems. Dr. Wakayama is a member of the Institute of Electronics, Information and Communication Engineers (IEICE) of Japan. He was a recipient of the IEICE Communications Society OCS Young Researcher's Award in 2015, the Best Paper Award of OECC 2016, and the Young Researcher's Award of IEICE in 2017.

Seiya Sumita received an M.E. degree in electrical and computer engineering from Yokohama National University, Yokohama, Japan, in 2011. After graduation, he joined KDDI Corporation, Tokyo, Japan. Since then, he has been involved in research and development on path computation and provisioning system of optical networks at KDDI R&D Laboratories Inc. (currently KDDI Research Inc.).

Hidenori Takahashi (M'08) received B.E. and M.E. degrees in electronic engineering from Tohoku University, Sendai, Japan, in 1998 and 2000, and a Ph.D. degree from Waseda University, Tokyo, Japan in 2012. He joined KDD R&D Laboratories Inc. (currently KDDI Research, Inc.) in 2000. He was involved in the research and development of silica-based planar waveguide devices. From 2006 to 2007, he was a Visiting Researcher and a Fellow of the Advanced Study Program with Massachusetts Institute of Technology, Cambridge, MA, USA. Since 2007, he has worked in highly spectrally efficient transmission systems with digital coherent optical OFDM technologies and high-capacity systems using multicore fiber. Since 2012, he has been a member of the Submarine Cable Planning and Engineering Section of KDDI Corporation. Since 2016, he has also been a member of the Photonic Transport Network Laboratory of KDDI Research, Inc., to realize future high-capacity and long-distance optical fiber transmission systems. Dr. Takahashi was a recipient of the Best Paper Award from the 7th International Conference on Optical Internet.

Noboru Yoshikane joined KDD (currently KDDI Corporation), Japan, in 1999, and since 2001 has been working at KDDI Research. Dr. Yoshikane has been engaged in research on the design of submarine cable systems, highly spectrally efficient optical communication systems using wavelength-division multiplexing transmission, and the design and modeling of photonic networks.

Itsuro Morita (F'21) received B.E., M.E., and Dr. Eng. degrees in electronics engineering from the Tokyo Institute of Technology, Tokyo, Japan, in 1990, 1992, and 2005, respectively. He joined Kokusai Denshin Denwa (KDD) Company, Ltd. (currently KDDI Corporation), Tokyo, in 1992, where he has been with the Research and Development

Laboratories since 1994. He has been engaged in research on long-distance and high-speed optical communication systems. In 1998, he was on leave at Stanford University, Stanford, CA, USA. He is currently the Principal Research Engineer of KDDI Research, Inc., and a Fellow of the IEICE. Dr. Morita was a recipient of the Minister Award from METI in 2006 and the Hisoka Maejima Award from the Tsushinbunka Association in 2011.

Takehiro Tsuritani (SM'21) received M.E. and Ph.D. degrees in electronics engineering from Tohoku University, Miyagi, Japan, in 1997 and 2006, respectively. He joined Kokusai Denshin Denwa (KDD) Company, Limited (currently KDDI Corporation), Tokyo, Japan, in 1997. Since 1998, he has been with their Research and Development Laboratories (currently KDDI Research, Inc.) and has been engaged in research on high-capacity long-haul wavelength division-multiplexed (WDM) transmission systems and dynamic photonic networking. He is currently an executive director, KDDI Research, Inc., and an IEICE Fellow. He was a recipient of the Best Paper Award of OECC 2000.

Masatoshi Suzuki (F'06) received B.E., M.E., and Ph.D. degrees from Hokkaido University, Sapporo, Japan, in 1979, 1981, and 1984, respectively. He joined KDD (currently KDDI), Tokyo, Japan, in 1984. Since then, he has been engaged in research on high-speed optical modulator-/laser-integrated devices, optical soliton transmission systems, WDM transmission systems, and optical networks, including pioneering works such as the first demonstration of a high-speed monolithically integrated modulator/laser light source in 1987 and the new proposal and demonstration of a dispersion-managed soliton transmission scheme in 1995. He was involved in the development of 10-Gbit/s WDM ultralong-distance transmission systems and demonstrated 10-Gbit/s RZ pulse-based WDM transmission over transoceanic distance in 1998, which were applied to transpacific and transatlantic undersea cable systems, such as Japan-US and TAT-14. He was the Executive Vice President of KDDI R&D Laboratories, Inc., from 2011 to 2016 and an R&D Fellow of KDDI Corporation from 2007 to 2017. He is currently the Principal Research Engineer of KDDI Research, Inc. His current research interests include wireless and optical integrated technology for future mobile networks and ultra large-capacity optical communication systems based on space-division multiplexing. He is a Fellow of the OSA and IEICE and a member of the Engineering Academy of Japan. He was an Associate Editor of the Journal of Lightwave Technologies from 1999 to 2004. Dr. Suzuki was a recipient of the Best Paper Award from OEC1988, OECC2010, and IEICE in 1996, the Achievement Award from IEICE in 2004, the Minister Award from MEXT (Ministry of Education, Culture, Sports, Science and Technology of Japan) in 2006, the Minister Award from METI (Ministry of Economy, Trade and Industry of Japan) in 2006, the Kenjiro Sakurai Memorial Prize from OITDA in 2009, the Hisoka Maejima Award from the Tsushinbunka Association in 2011, and the Medal with Purple Ribbon from Japan in 2017.